Preparation of Gold Nanoplates Using Ortho Carbonyl Compounds as Capping Agents for Electrochemical Sensing of Lead Ions

Xinde Jiang (jxd@nit.edu.cn)
Nanchang Institute of Technology https://orcid.org/0000-0003-3758-3863
Jianye Ma
Nanchang Institute of Technology
Guixian Jiang
Nanchang Institute of Technology
Manqing Xu
Nanchang Institute of Technology
Xueping Huang
Nanchang Institute of Technology
Guiqing Gao
Nanchang Institute of Technology
Xin Dai
Nanchang Institute of Technology

Nano Express

Keywords: nanoparticle, organic compounds, electrochemistry, waste water

Posted Date: October 5th, 2020

DOI: https://doi.org/10.21203/rs.3.rs-84468/v1

Version of Record: A version of this preprint was published at Nanoscale Research Letters on April 7th, 2021. See the published version at https://doi.org/10.1186/s11671-021-03521-2.

Abstract

In this study, gold nanoplates were synthesized using plant molecules (gallic acid) following a kinetic control mode. The growth of nanoplates is mainly due to the specific adsorption of capping agents on certain crystal facets. Through systematical characterizations, it is found that the distance between two oxygen atoms in ortho carbonyl compounds matches well with the lattice spacing of gold (111) facets exactly, which is beneficial to the formation of twin seeds and further the growth of plate-like gold nanoparticles. The gold nanoplates on glassy carbon electrode shows a remarkably improved electrochemical sensing activity of lead ions compared to the bare glassy carbon electrode or spherical gold nanoparticle modified electrode. The modified electrode is expected to be used in the detection of lead ion concentration in heavy metal wastewater.

Introduction

Thanks to the localized surface plasmon resonance (LSPR) property [1-4], gold nanoparticles have found many optical and electrochemical applications, including sensing, Raman spectroscopy, biological imaging, catalysis, biomedicine, and so forth[5-9]. The plasma properties of gold nanoparticles depend on their shape, size, composition and dielectric environment, especially the near-field enhancement of anisotropic gold nanoparticles is often highly amplified due to their sharp structural characteristics [10, 11]. In various morphologies, two-dimensional gold nanoplates have attracted much attention due to their unique optical properties, high conductivity, thermal stability and catalytic activity [12-14]. In the past few decades, a series of preparation methods have been developed to synthesis two-dimensional gold nanoplates, including photochemical reaction method, thermal decomposition method, seed-mediated method, microwave-assisted method and ultrasonic-assisted method [15-19]. However, most of these synthesis methods are not environmental friendly as they often involve the use of many surfactants or capping agents, chemical reducing agents, etc [20-22].

In recent years, the vigorous development of green chemistry has promoted the preparation of gold nanoplates by biological method [23]. Biomass such as lemongrass, *aloe vera*, seaweed, alfalfa, *E. coli* and *Platycladus orientalis* extract have been used as reductive and protective agents to synthesize gold nanoplates[24, 25]. For example, Shankar *et al* [26] developed a biological method to produce up to 45% gold nanoplates by citronella leaf extract. Montes *et al*[27] successfully prepared anisotropic gold nanoplates with size of 500-4000 nm and thickness of 15-30 nm by reducing $HAuCl_4$ solution with the aqueous extract of alfalfa. Zhan *et al*[28] reported a new method for the synthesis of gold nanoplates, i.e., the biological reduction of $HAuCl_4$ by using *Platycladus orientalis* extract with a kinetic control instrument. It is worth mentioning that the yield of gold nanoplates can be tuned by adjusting the experimental parameters, such as the feeding way/rate of the reagent, or the temperature and pH of the feed solution. For example, when the pH was 2.81 and the temperature was 60 ℃, the yield of gold nanoplates could be up to 39% by injecting *Platycladus orientalis* extract into the gold precursor at a speed of 60 $mL \cdot h^{-1}$.

It is difficult to give the exact mechanism of the nucleation and growth of gold nanoparticles in biosynthesis because the real active molecules in plant extracts are difficult to distinguish [29]. In previous studies, it was found that polyphenols play an important role in the formation of gold nanoplates [30]. In this study, gallic acid as a representative of polyphenols was used to study the growth mechanism of gold nanoparticles. Through a wide spectrum of structural characterizations, the role of ortho carbonyl compounds in the growth of gold nanoclusters into twins seeds and then plate-like nanoparticles was identified.

1. Material And Methods

1.1 Material

Chloroauric acid, gallic acid, sodium oxalate, ascorbic acid and lead sulfate are all analytical pure and purchased from Aladdin Chemical Reagent Co., Ltd.

1.2 Preparation of gold nanoplates

In a typical synthesis of gold nanoplates, a two-neck flask (50 mL) containing 10 mL Chloroauric acid (1.0 mmol·L^{-1}) was preheated in an oil bath (equipped with magnetic stirring) at 30 °C for 5 min. Feed solutions (gallic acid, 0.6 mmol·L^{-1}, 10 mL) were simultaneously injected into the flask through syringe pump (Shenzhen medical equipment technology development Co., Ltd., SK-500 Ⅱ, China) at the addition rate of 0.5, 1.0, 1.5, 2.0 and 2.5 mL·min^{-1}, respectively. The reaction mixture was maintained stirring for an additional 30 min after the completion of feeding.

1.3 Characterization

The UV-Vis spectrum of gold nanoparticles was measured by UV-Vis spectrophotometer (TU-1900, Beijing Purkinje General Instrument Co., Ltd., China) with water as reference, the scanning wavelength range was 330-800 nm, and the scanning step length was 1.0 nm. Transmission electron microscopy (TEM), high resolution transmission electron microscopy (HRTEM), selected area electron diffraction (SAED) and energy dispersive spectroscopy (EDS) were performed on a Phillips Analytical FEI Tecnai 30 electron microscope (300 kV). Fourier transform infrared spectrometer (FTIR) analysis was carried out by infrared spectrometer (Nicolet iS50, Nicolet company, USA), and the scanning wavenumber range was 400-4000 cm^{-1}. Thermogravimetry (TG) analysis was carried out in the thermogravimetry analyzer (TG209F1, Netzsch, Germany). The temperature range was 300-1000 ℃, the heating rate was 10 ℃·min^{-1}, and the air flow rate was 20 mL·min. The yield of the gold nanoplates was calculated by dividing the number of gold nanoplates by the total number of gold nanoparticles. In order to ensure the accuracy of the data, the number of nanoparticles analyzed was more than 1000.

1.4 Electrochemical sensing of lead ions

The glassy carbon electrode (3 mm in diameter) was polished with 0.03 and 0.05 μm alumina, and then washed by ultrasonication for 15 minutes in ethanol and ultra-pure water respectively. The as-prepared gold nanoparticles sol (100 uL) was drop-casted on the glassy carbon electrode, and dried in air. The casting of gold nanoparticles was repeated three times. The conditions of voltammetric test were: minimum voltage -2.0 V, maximum voltage 2.0 V, and scan rate 1 $mV \cdot S^{-1}$.

2. Results And Discussion

2.1Effect of feeding rate

In order to avoid the violent nucleation and growth of gold nanoparticles, the feeding rate of gallic acid was controlled by an injection pump, which consequently regulates the release rate of gold atoms during the reduction process. During the reaction, the concentration of gallic acid was fixed at 0.6 $mmol \cdot L^{-1}$, and the concentration of chloroauric acid wais 1.0 $mmol \cdot L^{-1}$. Gallic acid was injected into chloroauric acid solution. The total volume of the reaction solution was 20 mL, containing 10 mL gallic acid and 10 mL chloroauric acid solution, and the reaction temperature was 30 ℃. The feeding rates of gallic acid were 0.5, 1.0, 1.5, 2.0 and 2.5 $mL \cdot min^{-1}$, respectively. After feeding, the reaction continued at 30 ℃ for 30 minutes. The effect of feeding rate on the yield of gold nanoplates was investigated. As shown in Figure 1, as the feeding rate decreases, the surface plasmon resonance (SPR) peak of spherical gold nanoparticles gradually decreases, while a new absorption peak appears in the long wavelength region.

Figure 2 shows the transmission electron microscope (TEM) images of gold nanoparticles synthesized at different conditions. As the feeding rate decreases, the yield of the nanoplates increases from 0 to nearly 53%, and the side length of the nanoplates is about 500 nm. This result shows that a fast release of atoms is not conducive to heterogeneous nucleation, which requires twin seeds and suitable growth rate.

2.2Formation mechanism of gold nanoplates

As there were only gallic acid and chloroauric acid in the reaction system, its primary and secondary oxidation products (as shown in Scheme 1) might serve as capping reagents and induce the formation of gold nanoparticles. At the beginning of the reaction (with a feeding rate of 0.5 $mL \cdot min^{-1}$), chloroauric acid was excessive, gallic acid would be completely oxidized to ortho carbonyl compounds. Whereas at a high feeding rate (i.e. 2.5 $mL \cdot min^{-1}$), the gallic acid could be oxidized to enol compounds.

FTIR spectra of gallic acid, spherical and plate-like gold nanoparticles are shown in Figure 3. The peaks at 3496 and 1538 cm^{-1} in the spectrum of gallic acid correspond to the phenolic hydroxyl and benzene ring, which disappear in the spectra of both spherical and plate-like gold nanoparticles. This means that gallic acid would not absorb on the nanoparticles. The peaks at 1722 and 1618 cm^{-1} belong to carbonyl group and carbon-carbon double bonds are observed in both the spherical and plate-like gold nanoparticles. The difference is that the absorption of carbonyl group is much stronger in the plate-like nanoparticles. This

result indicates that the phenolic hydroxyl was oxidized to the enol structure (absorbed on spherical nanoparticles), and further to the ortho carbonyl compound (absorbed on plate-like nanoparticles).

In order to clarify the specific adsorption of ortho carbonyl on the gold nanoplates, the adsorbed molecules on the gold nanoplates were studied by EDS (Figure 4a). Except for Au element, only C and O are found on the surface of gold nanoplates. The ratio of C to O on the surface of the gold nanoplates measured by EDS is 6.8:5 (815:599), close to that in gallic acid ($C_7H_6O_5$) is 7:5. This indicates that the molecules on the surface of the gold nanoplates are mainly from the oxidation products of gallic acid. TG analysis was conducted to examine the residual molecules on the gold nanoplates. Evidently, Figure 4b shows that the biomass accounts for 5.6 % of the total weight of the gold nanoplates. The decomposition temperature of the biomass is in the range of 400–700 K, in accordance with that of organic matter [31]. This result suggests that the biomass adheres to gold nanoparticles as a thin layer and acts as protective agents that prevent the aggregation of the gold nanoparticles, which is in agreement with a previous report [32].

As we know, the lattice spacing of different crystal planes is different. For example, the lattice spacing of Au (111) plane is 0.234 nm, and that of (100) plane is 0.204 nm, and the lattice spacing of (110) plane is 0.144 nm. Because of the different arrangement angles between atoms, the bond lengths formed by atoms on different crystal planes are also different. Au (111) plane is the most closely arranged, resulting in the least electronic defects, so the crystal plane energy is the lowest. In this study, the calculated distance between two rows of gold atoms is 0.234 nm (Figure 5).

The primary and secondary oxidation products of gallic acid both have carboxyl and carbonyl group, the difference is that the latter have ortho carbonyl groups. The bond length of C-C single bond and C=O double bond are 0.15 and 0.12 nm respectively, whereas the four atoms of ortho carbonyl group form an isosceles trapezoid with a 60° base angle (Figure 6). Therefore, the distance between the two oxygen atoms can be calculated to be 0.27 nm, which matches the atomic distance of Au (111) planes. This result confirms that the ortho carbonyl group would preferentially adsorb on the surface Au (111) planes to form twin seeds.

2.3Preparation of gold nanoplates with ortho carbonyl compounds as capping agents

To further investigate the effect of ortho carbonyl on the formation of gold nanoplates, sodium oxalate with similar structure was used as a protective agent and ascorbic acid as a reducing agent to prepare gold nanoparticles. When the concentration of ascorbic acid was 0.4 $mmol{\cdot}L^{-1}$ and the concentration of gold precursor was 1.0 $mmol{\cdot}L^{-1}$. The as-prepared nanoparticles were characterized by UV-Vis spectroscopy (Figure 7a). As the concentration of sodium oxalate increases from 0.1 to 0.6 $mmol{\cdot}L^{-1}$, the absorption peak of spherical nanoparticles decreases gradually, while the absorption in the long wavelength region increases gradually. Through the TEM characterization, it can be found that when the concentration of sodium oxalate was 0.6 $mmol{\cdot}L^{-1}$, most of the obtained nanoparticles possessed a plate-like morphology (Figure 7b).

2.4 Electrochemical sensing of lead ions

The glassy carbon electrode (3 mm in diameter) was polished with 0.3 and 0.05 μm slurry and then ultrasonicated for 3 minutes in ethanol and ultra-pure water respectively, and dried in N_2. Linear sweep voltammetry test was conducted with glassy carbon electrode (modified with gold nanoparticles) as the working electrode, a platinum wire as counter electrode and a Ag-AgCl electrode as reference electrode. The conditions of voltammetry test were: minimum voltage -2.0 V; maximum voltage 2.0 V; scan rate 1 $mV \cdot S^{-1}$. The electrochemical response of plate-like nanoparticles, spherical nanoparticles and the bare glassy carbon electrodes to lead ions is shown in Figure 8. It can be found that the current response of plate-like nanoparticles to lead ions concentration shows a high linearity (R^2 = 0.9970, Figure 8a). Whereas for the spherical gold nanoparticles, the linearity between the concentration and the current value is lower (R^2 = 0.9874, Figure 8b). The bare glassy carbon electrode shows an even lower linearity (R^2 = 0.9704, Figure 8c) between the concentration and the current in the concentration range of 1000 - 10 $mg \cdot L^{-1}$. What is more, the current response of bare glassy carbon electrode is much weaker than that of electrodes loaded with gold nanoparticles. The plate-like gold nanoparticles have active edges and therefore show amplified signals in the lead ion solution [33, 34]. The durability of gold nanoplates modified glassy carbon electrode was further evaluated in the electrochemical test of lead ions after being placed at ambient atmosphere for 3 weeks. As shown in Figure 8d, the relationship between the concentration and the current remains a high linearity (R^2 =0.9934), and this modified electrode is expected to be used in the detection of lead ion concentration in heavy metal wastewater.

3. Conclusions

In conclusion, gold nanoplates have been synthesized by plant molecules. The formation of nanoplates is mainly due to the specific adsorption of ortho carbonyl compounds on the gold (111) facets. The distance between two oxygen atoms matches well with the spacing of gold (111) facet, which is beneficial to the formation of twin seeds and further the growth of plate-like gold nanoparticles. Due to the distinctive "edge effect" of gold nanoplates, the signal of lead ions in the linear sweep voltammetry test is much stronger than that of the bare electrode or spherical gold nanoparticle modified electrode. The developed gold nanoplates are expected to be used in the detection of lead ion concentration in heavy metal wastewater.

Declarations

Acknowledgements:

This project was financially supported by Natural Science Foundation of China (21706113) and Natural Science Foundation of Jiangxi Provincial Department of Education (GJJ190947).

Conflict of Interest:

The authors declare that they have no conflict of interest.

References

[1] Stewart M E, Anderton C R, Thompson L B, Maria J, Gray S K, Rogers J A, Nuzzo R G. Nanostructured plasmonic sensors. Chem Rev. 2008; 108(2): 494-521.

[2] Morarescu R, Shen H H, Vallee R A L, Maes B, Kolaric B, Damman P. Exploiting the localized surface plasmon modes in gold triangular nanoparticles for sensing applications. J Mater Chem. 2012; 22(23): 11537-11542.

[3] Major T A, Devadas M S, Lo S S, Hartland G V. Optical and dynamical properties of chemically synthesized gold nanoplates. J Phys Chem C. 2013; 117(3): 1447-1452.

[4] Jain P K, Huang X, El-Sayed I H, El-Sayed M A. Noble metals on the nanoscale: optical and photothermal properties and some applications in imaging, sensing, biology, and medicine. Accounts Chem Res. 2008: 41(12): 1578-1586.

[5] Sun M, Zhai C, Hu J, Zhu M, Pan J. Plasmon enhanced electrocatalytic oxidation of ethanol and organic contaminants on gold/copper iodide composites under visible light irradiation. J Colloid Inter Sci. 2018: 511: 110-118.

[6] Ye P, Xin W, De Rosa I, Wang Y, Goorsky M, Zheng L, Yin X, Xie Y. One-pot self-templated growth of gold nanoframes for enhanced surface-enhanced raman scattering performance. ACS Appl Mater Inter. 2020; 12(19): 22050-22057.

[7] Mohammad A M, Al-Akraa I M, El-Deab M S. Superior electrocatalysis of formic acid electro-oxidation on a platinum, gold and manganese oxide nanoparticle-based ternary catalyst. Int J Hydrogen Energ. 2018; 43(1): 139-149.

[8] Saha K, Agasti S S, Kim C, Li X, Rotello V M. Gold nanoparticles in chemical and biological sensing. Chem Rev. 2012; 112(5): 2739-2779.

[9] Dreaden E C, Alkilany A M, Huang X, Murphy C J, El-Sayed M A. The golden age: gold nanoparticles for biomedicine. Chem Soc Rev. 2012; 41(7): 2740-2779.

[10] Imaeda K, Hasegawa S, Imura K. Static and dynamic near-field measurements of high-order plasmon modes induced in a gold triangular nanoplate. J Phys Chem Lett. 2018; 9(14): 4075-4081.

[11] Jans H, Huo Q. Gold nanoparticle-enabled biological and chemical detection and analysis. Chem Soc Rev. 2012; 41: 2849-2866.

[12] Imaeda K, Hasegawa S, Imura K. Imaging of plasmonic eigen modes in gold triangular mesoplates by near-field optical microscopy. J Phys Chem C. 2018; 122(13): 7399-7409.

[13] Leonardo S, Coronado-Puchau M, Giner-Casares J J, Langer J, Liz-Marza´n L M. Monodisperse gold nanotriangles: size control, large-scale self-assembly, and performance in surface-enhanced raman scattering. ACS Nano. 2014; 8(6): 5833–5842.

[14] Hwang A, Kim E, Moon J, Lee H, Lee M, Jeong J, Lim E K, Jung J, Kang T, Kim B. Atomically flat Au nanoplate platforms enable ultraspecific attomolar detection of protein biomarkers. ACS Appl Mater Inter. 2019; 11(21): 18960-18967.

[15] Millstone J E, Wei W, Jones M R, Yoo H J, Mirkin C A. Iodide ions control seed-mediated growth of anisotropic gold nanoparticles. Nano Lett. 2008; 8(8): 2526-2529.

[16] Xin W, Severino J, De Rosa I M, Yu D, McKay J, Ye P, Yin X, Yang J M, Carlson L, Kodambaka S. One-step synthesis of tunable-size gold nanoplates on graphene multilayers. Nano Lett. 2018; 18(3): 1875-1881.

[17] Yang F, Huang J, Odoom-Wubah T, Hong Y, Du M, Sun D, Jia L, Li Q. Efficient Ag/CeO_2 catalysts for CO oxidation prepared with microwave-assisted biosynthesis. Chem Eng J. 2015; 269: 105-112.

[18] Shaik F, Zhang W, Niu W. A novel photochemical method for the synthesis of Au triangular nanoplates inside nanocavity of mesoporous silica shells. J Phys Chem C. 2017; 121(17): 9572-9578.

[19] Nori N M, Abdi K, Khoshayand M R, Ahmadi S H, Lamei N, Shahverdi A R. Microwave-assisted biosynthesis of gold-silver alloy nanoparticles and determination of their Au/Ag ratio by atomic absorption spectroscopy. J Exp Nanosci. 2013; 8(4): 442-450.

[20] Personick M L, Mirkin C A. Making sense of the mayhem behind shape control in the synthesis of gold nanoparticles. J Am Chem Soc. 2013; 135(49): 18238-18247.

[21] Hormozi-Nezhad M R, Karami P, Robatjazi H. A simple shape-controlled synthesis of gold nanoparticles using nonionic surfactants. Rsc Adv. 2013; 3(21): 7726-7732.

[22] Moon S Y, Kusunose T, Sekino T. CTAB-assisted synthesis of size- and shape-controlled gold nanoparticles in SDS aqueous solution. Mater. Lett. 2009; 63(23): 2038-2040.

[23] Iravani S. Green synthesis of metal nanoparticles using plants. Green Chem. 2011; 13(10): 2638-2650.

[24] Mazdeh S K, Motamedi H, Khiavi A A, Mehrabi M R. Gold nanoparticle biosynthesis by *E. coli* and conjugation with streptomycin and evaluation of its antibacterial effect. Curr Nanosci. 2014; 10(4): 553-561.

[25] Huang J, Li Q, Sun D, Lu Y, Su Y, Yang X, Wang H, Wang Y, Shao W, He N, Hong J, Chen C. Biosynthesis of silver and gold nanoparticles by novel sundried *Cinnamomum camphora* leaf. Nanotechnology. 2007; 18(10): 105104.

[26] Shankar S S, Rai A, Ankamwar B, Singh A, Ahmad A, Sastry M. Biological synthesis of triangular gold nanoprisms. Nat Mater. 2004; 3(7): 482-488.

[27] Montes M O, Mayoral A, Deepak F L, Parsons J G, Jose-Yacaman M, Peralta-Videa J R, Gardea-Torresdey J L. Anisotropic gold nanoparticles and gold plates biosynthesis using alfalfa extracts. J Nanopart Res. 2011; 13(8): 3113-3121.

[28] Zhan G, Ke L, Li Q, Huang J, Hua D, Ibrahim A R, Sun D. Synthesis of gold nanoplates with bioreducing agent using syringe pumps: a kinetic control. Ind Eng Chem Res. 2012; 51(48): 15753-15762.

[29] Zhou Y, Lin W, Yang F, Fang W, Huang J, Li Q. Insights into formation kinetics of gold nanoparticles using the classical JMAK model. Chem Phys. 2014; 441: 23-29.

[30] Jiang X, Sun D, Zhang G, He N, Liu H, Huang J, Odoom-Wubah T, Li Q. Investigation of active biomolecules involved in the nucleation and growth of gold nanoparticles by *Artocarpus heterophyllus Lam* leaf extract. J Nanopart Res. 2013; 15(6): 1741.

[31] Huang J, Wang W, Lin L, Li Q, Lin W, Li M, Mann S. A general strategy for the biosynthesis of gold nanoparticles by traditional chinese medicines and their potential application as catalysts, Chem-Asian J. 2009; 4(7): 1050-1054.

[32] Ah C S, Yun Y J, Park H J, Kim W J, Ha D H, Yun W S. Size-controlled synthesis of machinable single crystalline gold nanoplates. Chem Mater. 2005; 17(22): 5558-5561.

[33] Xu X, Luo J, Liu M, Wang Y, Yi Z, Li X, Yi Y, Tang Y. The influence of edge and corner evolution on plasmon properties and resonant edge effect in gold nanoplatelets. Phys Chem Chem Phys. 2015; 17(4): 2641-2650.

[34] Xu X, Yi Z, Li X, Wang Y, Liu J, Luo J, Luo B, Yi Y, Tang Y. Tunable nanoscale confinement of energy and resonant edge effect in triangular gold nanoprisms. J Phys Chem C. 2013; 117(34): 17748-17756.

Scheme 1

Scheme 1 is available in the Supplementary Files.

Figures

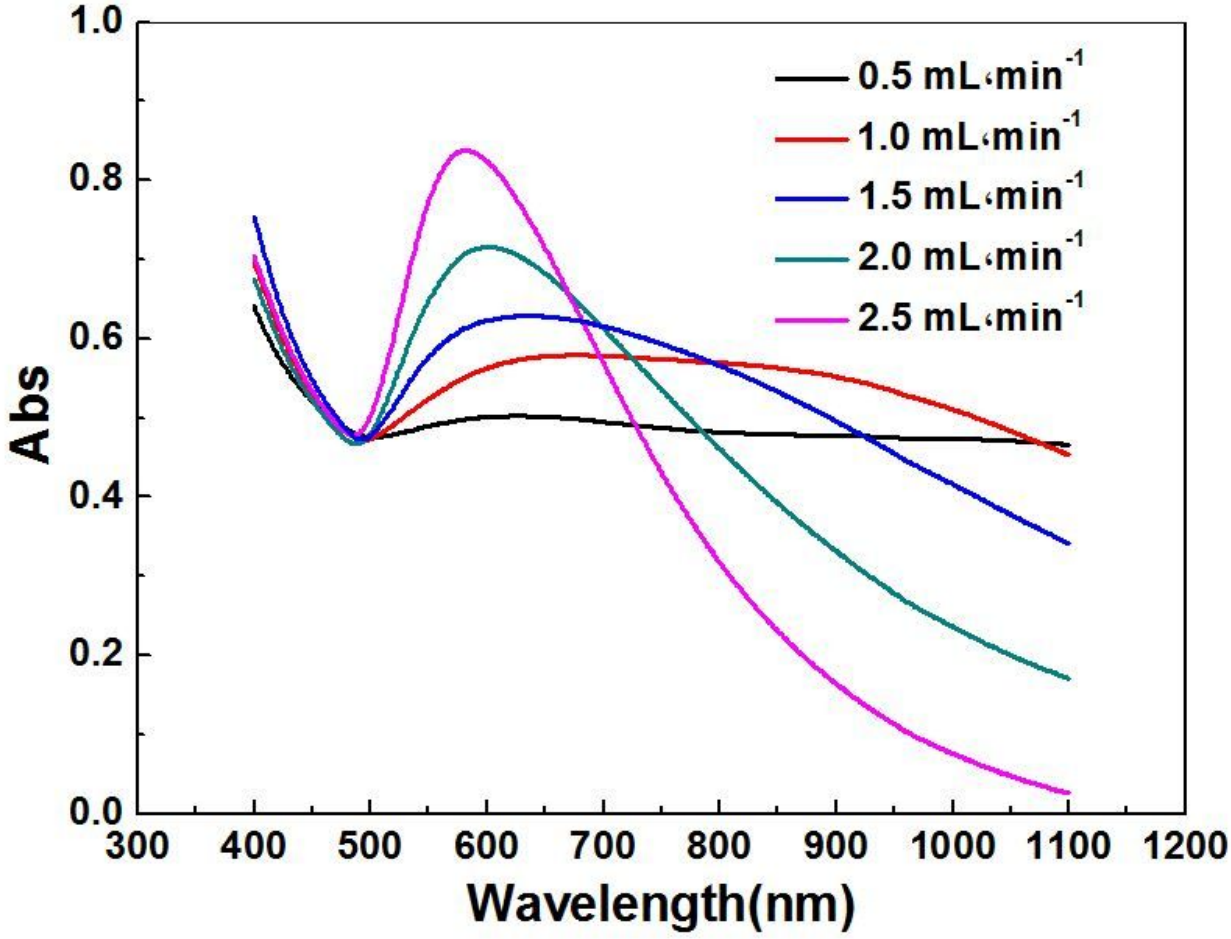

Figure 1

UV-Vis spectra of gold nanoparticles prepared with the feeding rate of 0.5, 1.0, 1.5, 2.0 and 2.5 mL·min-1

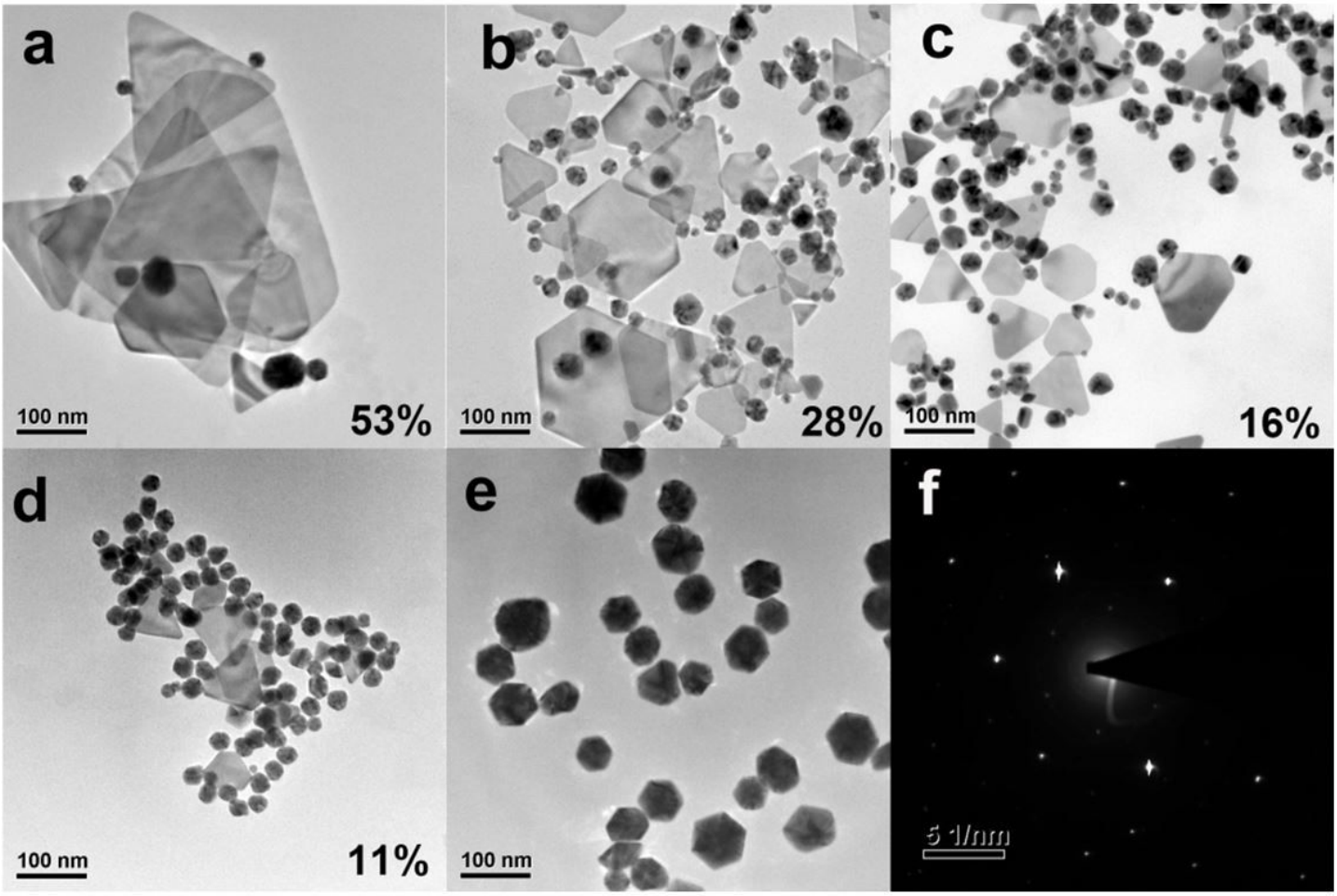

Figure 2

TEM characterizations of gold nanoparticles prepared with the feeding rate of 0.5, 1.0, 1.5, 2.0 and 2.5 mL·min-1 (a-e) and SAED pattern of gold nanoplates (f)

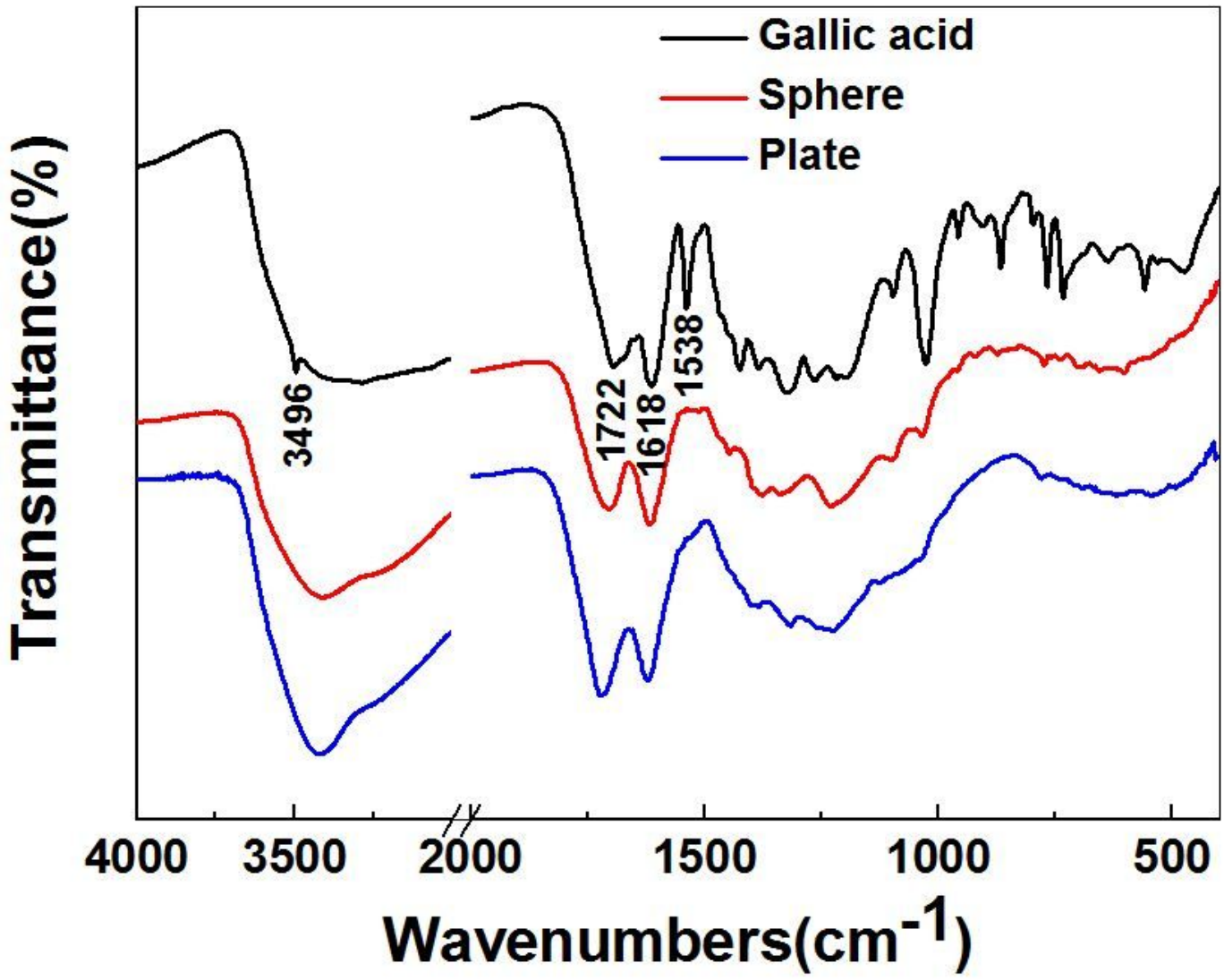

Figure 3

FTIR spectra of gallic acid, spherical and plate-like gold nanoparticles

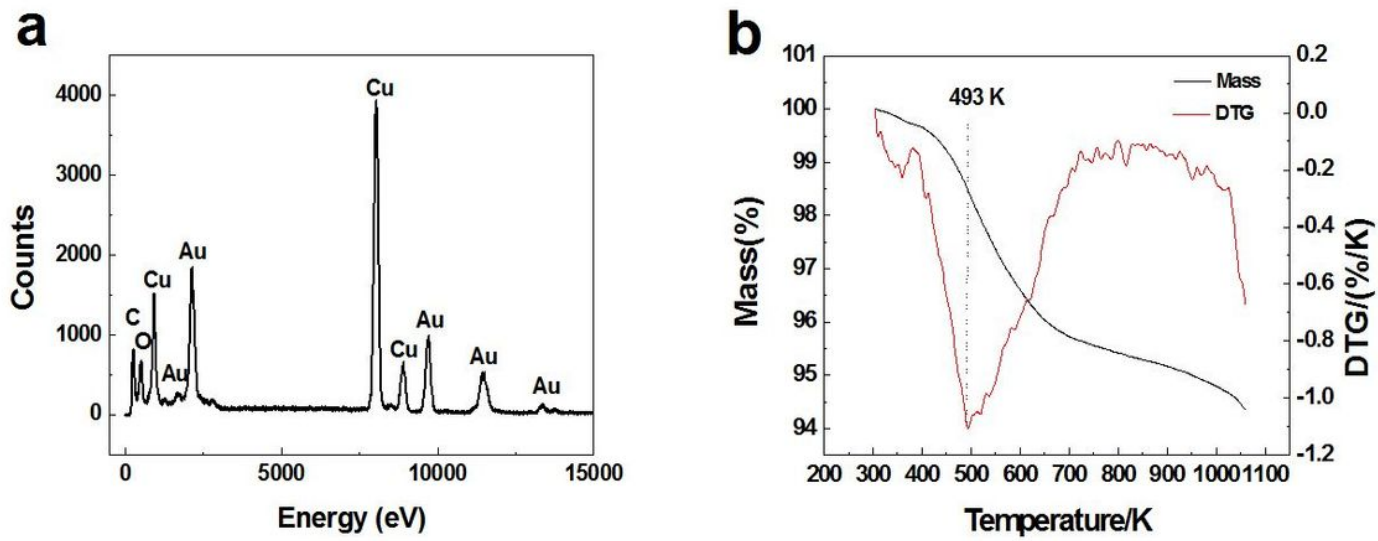

Figure 4

EDS spectrum (a) and TG (b) profiles of gold nanoplates

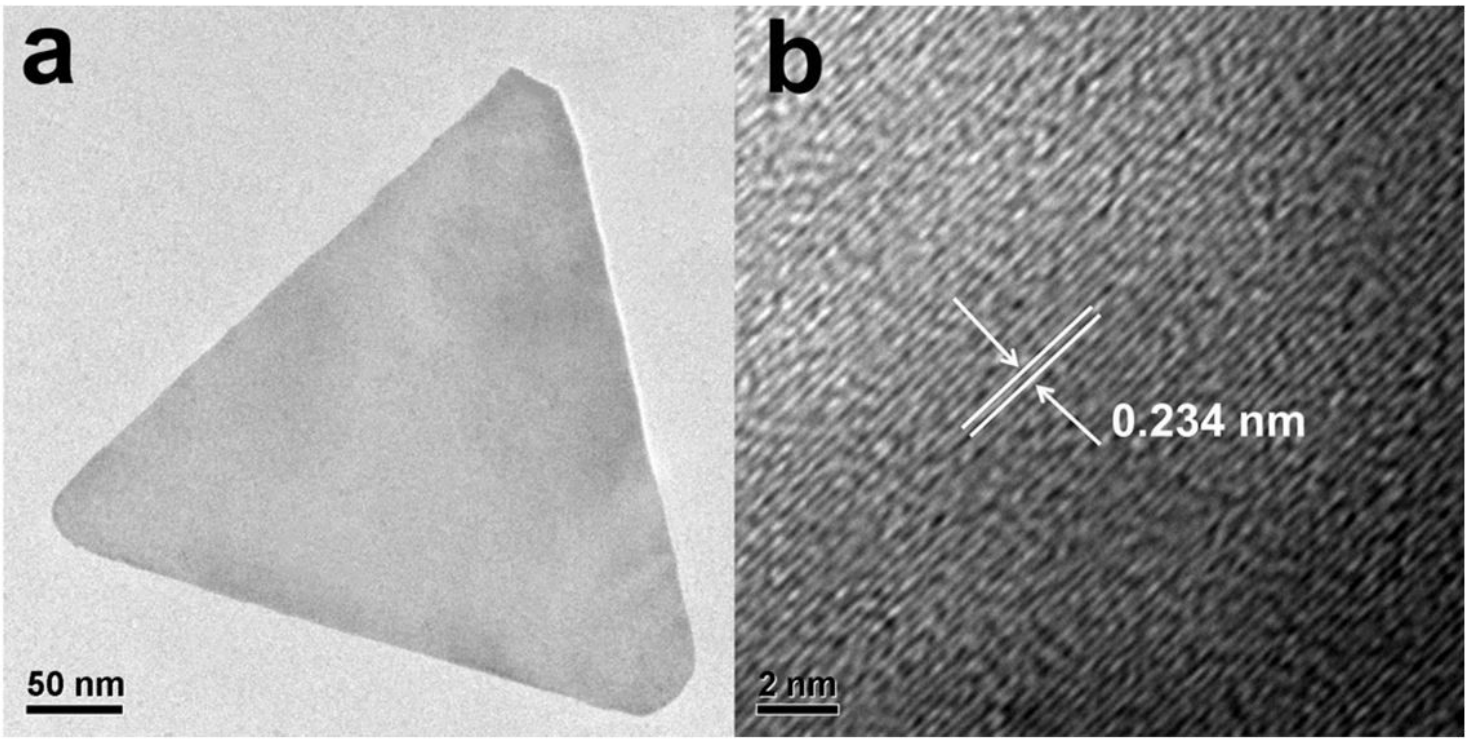

Figure 5

Typical TEM (a) and HRTEM (b) image of a single gold nanoplate

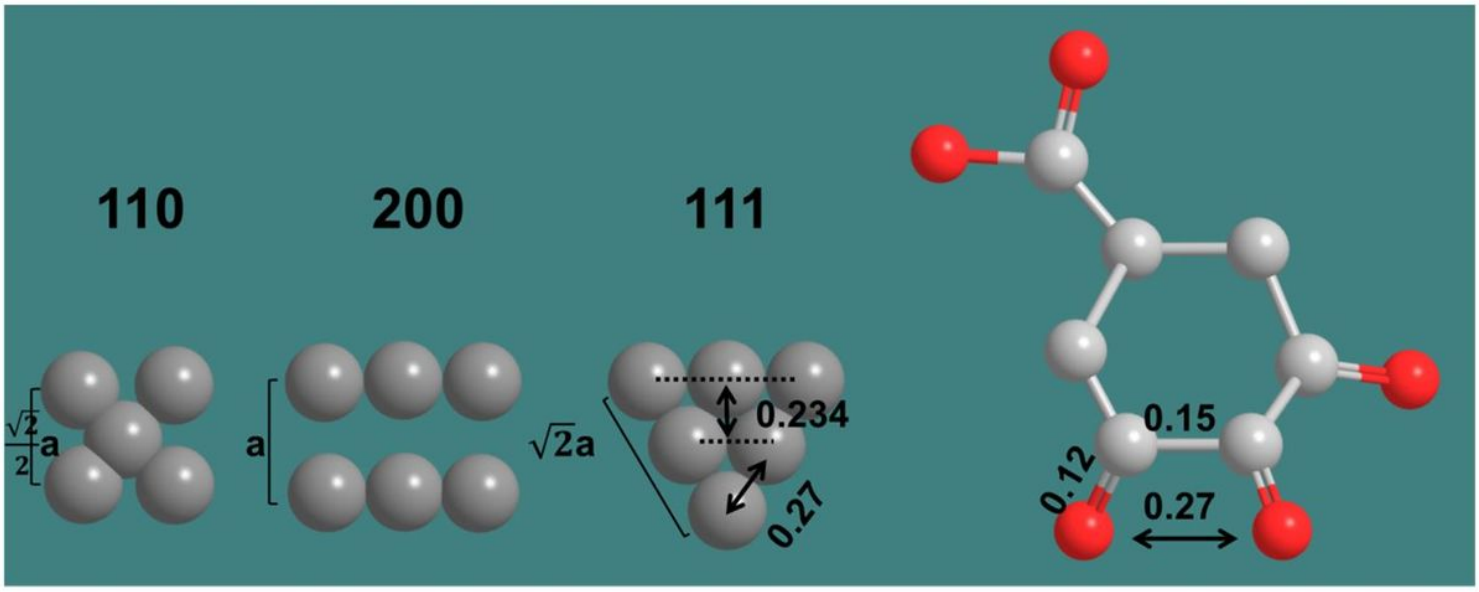

Figure 6

Schematic diagram of the preferential adsorption of capping reagents on Au (111) facet

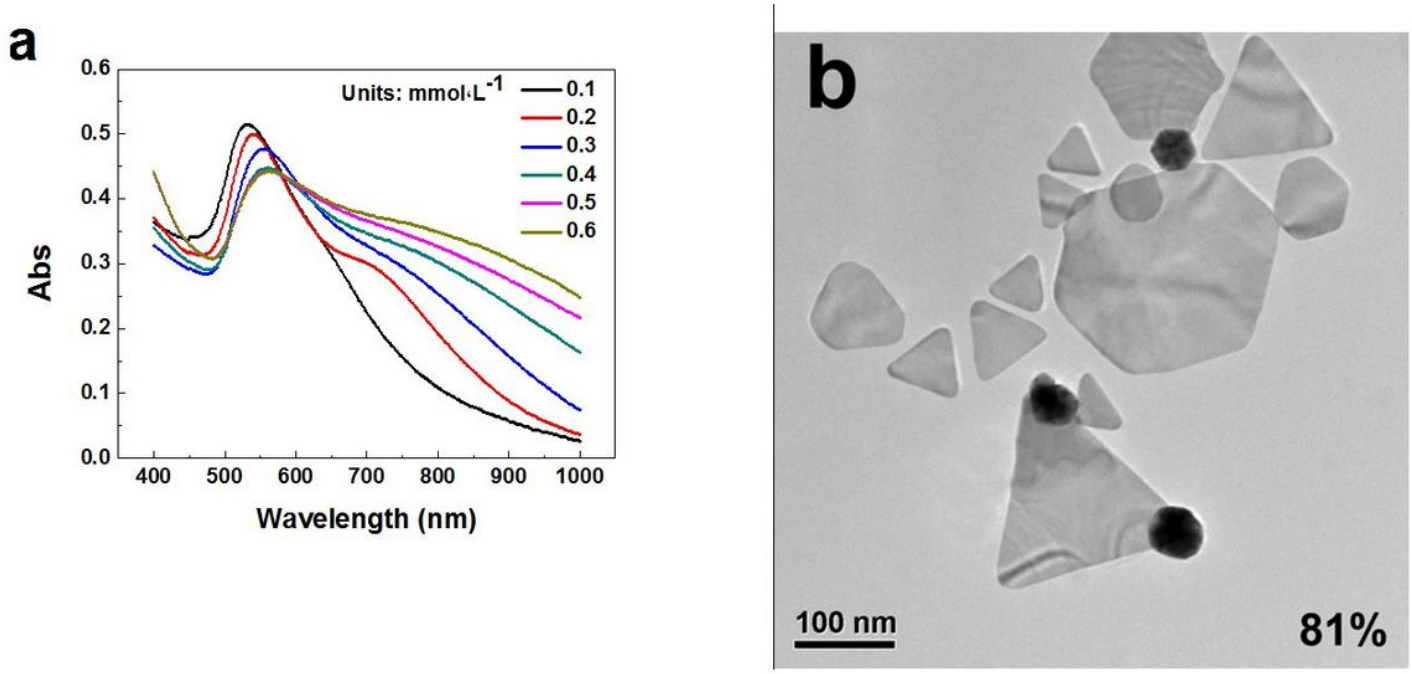

Figure 7

Preparation of gold nanoparticles with sodium oxalate as protective agent: (a) UV-Vis spectra; (b) TEM image

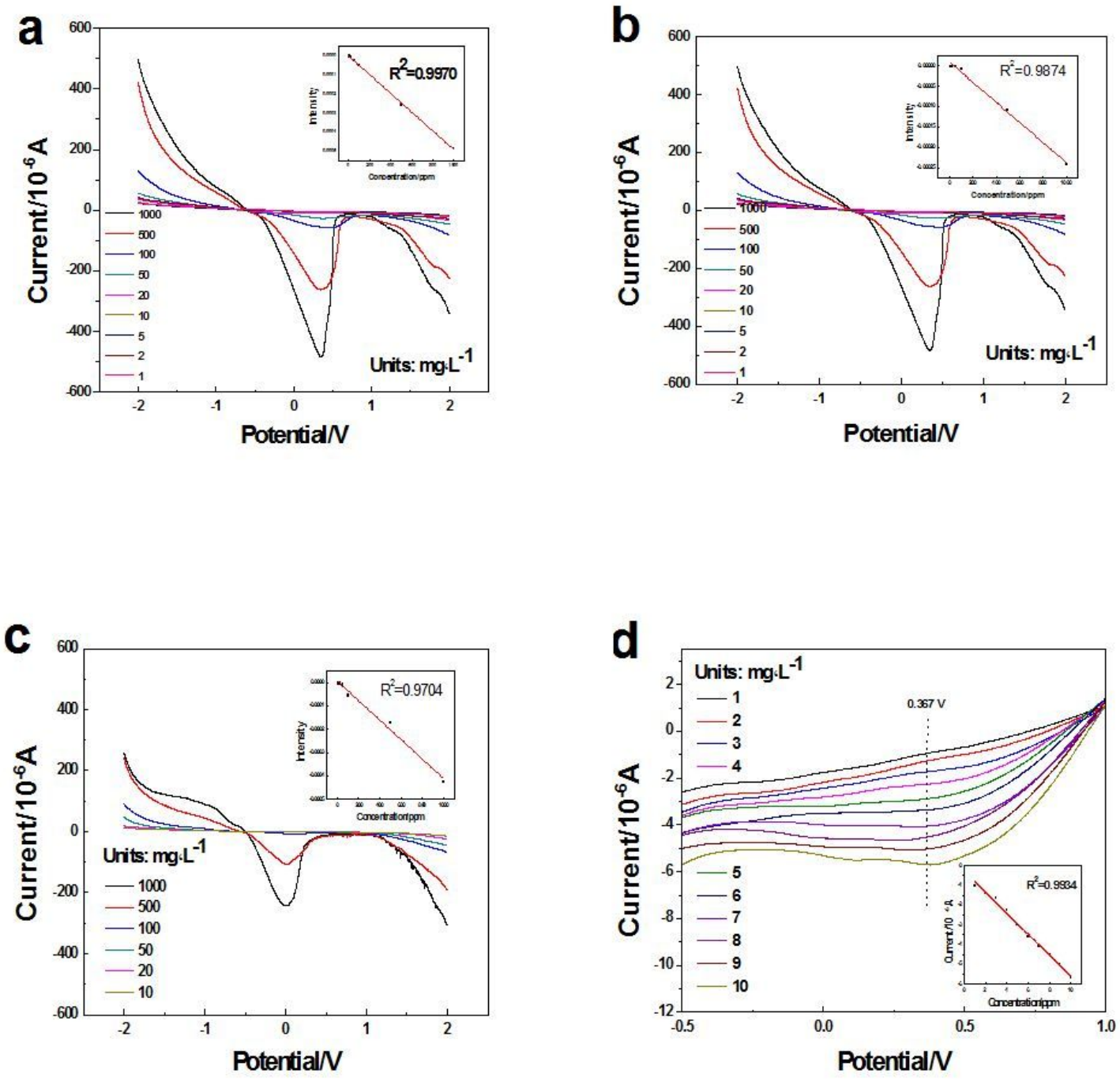

Figure 8

The application of gold nanoparticles in the detection of lead ions by electrochemical sensor

Supplementary Files

This is a list of supplementary files associated with this preprint. Click to download.

- Scheme1.JPG